Advanced Topographic Laser Altimeter System (ATLAS) Receiver Telescope Assembly (RTA) and Transmitter Alignment and Test.

John Hagopian, Matthew Bolcar, John Chambers, Allen Crane, Bente Eegholm,
Tyler Evans, Samuel Hetherington, Eric Mentzell,
Patrick Thompson, Luis Ramos-Izquierdo, David Vaughnn

National Aeronautic and Space Administration, Goddard Space Flight Center,
8800 Greenbelt Road, Greenbelt, MD, USA 20776

ABSTRACT

The sole instrument on NASA's ICESat-2 spacecraft shown in Figure 1 will be the Advanced Topographic Laser Altimeter System (ATLAS)[1]. The ATLAS is a Light Detection and Ranging (LIDAR) instrument; it measures the time of flight of the six transmitted laser beams to the Earth and back to determine altitude for geospatial mapping of global ice. The ATLAS laser beam is split into 6 main beams by a Diffractive Optical Element (DOE) that are reflected off of the earth and imaged by an 800 mm diameter Receiver Telescope Assembly (RTA). The RTA is composed of a 2-mirror telescope and Aft Optics Assembly (AOA) that collects and focuses the light from the 6 probe beams into 6 science fibers. Each fiber optic has a field of view on the earth that subtends 83 micro Radians. The light collected by each fiber is detected by a photomultiplier and timing related to a master clock to determine time of flight and therefore distance. The collection of the light from the 6 laser spots projected to the ground allows for dense cross track sampling to provide for slope measurements of ice fields. NASA LIDAR instruments typically utilize telescopes that are not diffraction limited since they function as a light collector rather than imaging function. The more challenging requirements of the ATLAS instrument require better performance of the telescope at the ¼ wave level to provide for improved sampling and signal to noise. NASA Goddard Space Flight Center (GSFC) contracted the build of the telescope to General Dynamics (GD). GD fabricated and tested the flight and flight spare telescope and then integrated the government supplied AOA for testing of the RTA before and after vibration qualification. The RTA was then delivered to GSFC for independent verification and testing over expected thermal vacuum conditions. The testing at GSFC included a measurement of the RTA wavefront error and encircled energy in several orientations to determine the expected zero gravity figure, encircled energy, back focal length and plate scale. In addition, the science fibers had to be aligned to within 10 micro Radians of the projected laser spots to provide adequate margin for operations on-orbit. This paper summarizes the independent testing and alignment of the fibers performed at the GSFC.

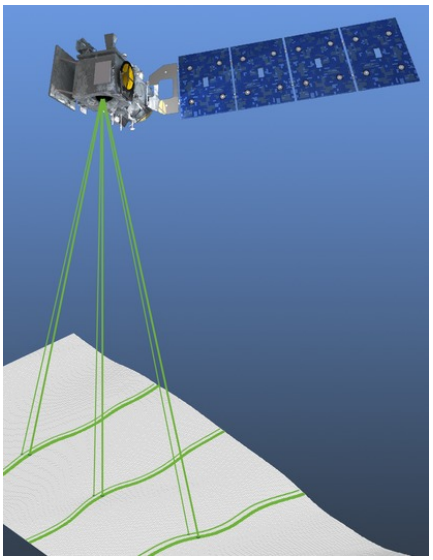

Figure 1. ICESat-2 Spacecraft

Keywords: ATLAS, Receiver Telescope Assembly, LIDAR, ICESat-2, Interferometry, Encircled Energy, Optical Test

1. INTRODUCTION

NASA GSFC has built a number of LIDAR instruments with increasingly challenging imaging and alignment requirements. The ATLAS instrument is designed to map Polar Ice and intervening clouds and vegetation. The ATLAS laser and spare produces about 9 Watts of equivalent CW power in pulses that last nanoseconds (the pulses are about 1 meter in length). The lasers have internal beam expanders followed by a reflective beam expander that further increase the beam diameters to about 45 millimeters and subtend approximately 20 micro Radians. The ATLAS telescope was manufactured by General Dynamics, the 0.8-meter light-weighted primary mirror was diamond turned then plated with

Earth Observing Systems XXI, edited by James J. Butler, Xiaoxiong (Jack) Xiong, Xingfa Gu, Proc. of SPIE
Vol. 9972, 997207 · © 2016 SPIE · CCC code: 0277-786X/16/$18 · doi: 10.1117/12.2240241

electroless nickel and polished with a small tool. The secondary mirror is also beryllium with electroless nickel plating. Both mirrors were then coated with enhanced aluminum for optimal performance at the 532-nanometer wavelength. The Aft Optics was designed assembled and tested at NASA GSFC using fused silica lenses fabricated by Optimax and then a narrow band transmission coating applied to minimize out of band stray light. The ATLAS telescope was originally specified to meet an encircled energy requirement of 80% encircled energy within 8.5 microns at the focal plane; but less than ideal substrate finish from diamond turning resulted in degraded but acceptable performance and created some challenges in predicting the encircled energy performance in zero gravity that had to be addressed. The encircled energy specification is a good measure of how tightly reflected light can be focused on the ATLAS focal plane, which consists of six 300 micron diameter fiber optics aligned to the back of the Aft Optics Assembly. In addition to the image quality required to provide a tight focused image, the fiber optics in the focal plane must be aligned to within 10 micro Radians of the transmitted laser beams. This paper details optical testing of the Receiver Telescope Assembly[2] and the alignment of the science fibers to achieve this tight transmitter to receiver co-boresight requirement.

2. RTA IMAGE QUALITY TESTING

2.1 RTA 0-G Wavefront Error

If the ATLAS RTA were infinitely stiff, we could verify the encircled energy requirement directly by imaging a diffraction-limited point source. Since it is not, we relied on a test and analysis approach that could remove the effects of RTA gravity and imperfections in our ground support equipment (GSE). The ATLAS RTA wavefront error was measured using a commercial interferometer in a double pass configuration using a large retro flat as shown in Figure 2.

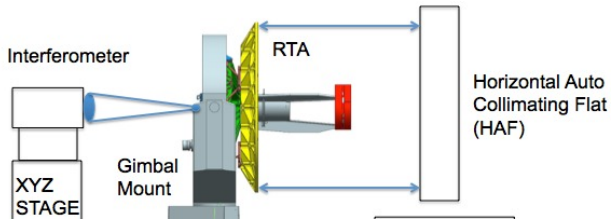

Figure 2. Double Pass Interferometry of RTA

The ATLAS RTA was mounted in a modified commercial gimbal mount that allows for precise anglular tip/tilt adjustment to allow measurement of the wavefront at select field points. The RTA is mounted on a diamond turned interface plate on the gimbal to control interface stress. The plate is diamond turned at the 3 RTA interface points and on the opposite face to allow access to an optical reference that is tied to datum that defines the RTA boresight. The gimbal mount was also fitted with a rotation stage to allow clocking of the RTA for alignment purposes and to allow the wavefront to be measured in multiple optical axis horizontal orientations to provide a 0-G wavefront map of the precise focal surface. Alignment of the interferometer to the RTA was performed by utilizing a Ball Alignment Fixture (BAF) that consists of a diamond turned flat with holes drilled at precise points that are populated with removable precision tooling balls that can be precisely positioned along focus relative to the diamond turned datum surface. Figure 3 shows the view from behind the RTA mounted in the gimbal. The BAF replaces the ATLAS focal plane plate that resides on the Aft Optics and is an alignment aid for positioning the interferometer and mapping out the RTA focal plane to allow placement of the flight optical fibers. In our test configuration the interferometer is mounted on a stage that is adjustable in the focus axis and horizontally to interrogate the instrument field of view. We employ a faster transmission sphere (lower f/#) on our interferometer to allow us to overfill the secondary mirror to eliminate the need to tilt the interferometer during wavefront testing across the field of view. To measure the wavefront

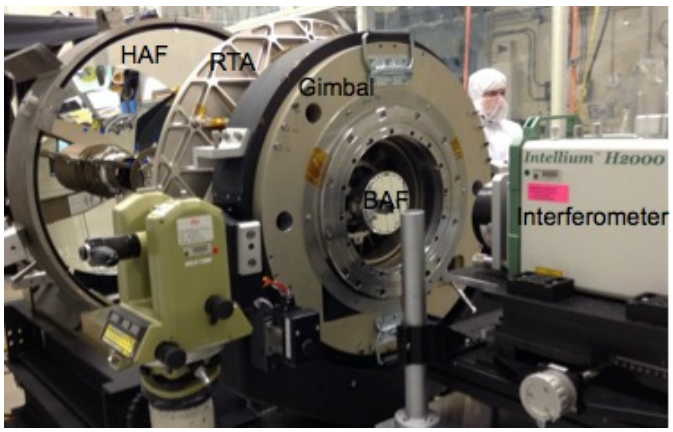

Figure 3. Interferometer viewing BAF, RTA and HAF

on-axis we merely measure the back of the RTA interface plate with a theodolite and align the retro flat to the same angle using another theodolite. With the ball plate installed, we initially tip/tilt the interferometer to the ball plate diamond turned surface (with a transmission flat) then we replace the transmission flat with the transmission sphere and translate the interferometer to the on-axis ball position (which is at a known distance from our reference datum on the AOA). After achieving a null on the ball, we remove the ball (which is precisely aligned in a delrin holder, which is aligned to the BAF datum); we note the initial axial and horizontal translation reading on the micrometers that are used to align the interferometer. The interferometer is then translated along the focus axis to minimize power in the RTA double pass wavefront and the new micrometer position noted and the wavefront recorded. We then proceed to the next field point by simply tilting the transmission flat in azimuth; for ATLAS we selected azimuth tilts that represent the radial offset of the inner and outer field points as well as the TAMS (Transmitter Alignment metrology System). The center and four off axis field points represent a slice of the focal surface. The HAF mirror figure is analytically subtracted from the wavefront map at each position.

2.2 RTA Zero Gravity RTA wavefront error

In order to interrogate the entire focal surface and measure the 0-G wavefront error we acquire and correct wavefront maps at each field position and at 60 degree clocking intervals. The RTA is clocked in the gimbal mount and wavefront measurements acquired at each field for each of these six clocking angles. At each RTA clocking angle the BAF is counter-rotated to allow field sampling to stay in the plane of the interferometer horizontal translator. Wavefront maps for 180 degree rotated pairs average out gravity-induced deformations. By processing and averaging the three 180 degree averaged pairs a zero gravity figure can be estimated. This allows independent verification of the measurements performed at General Dynamics with the telescope offloaded by mechanical paddles. Figure 4 shows the individual and processed wavefront maps for the three 180 degree-clocking pairs after the HAF mirror has been subtracted.

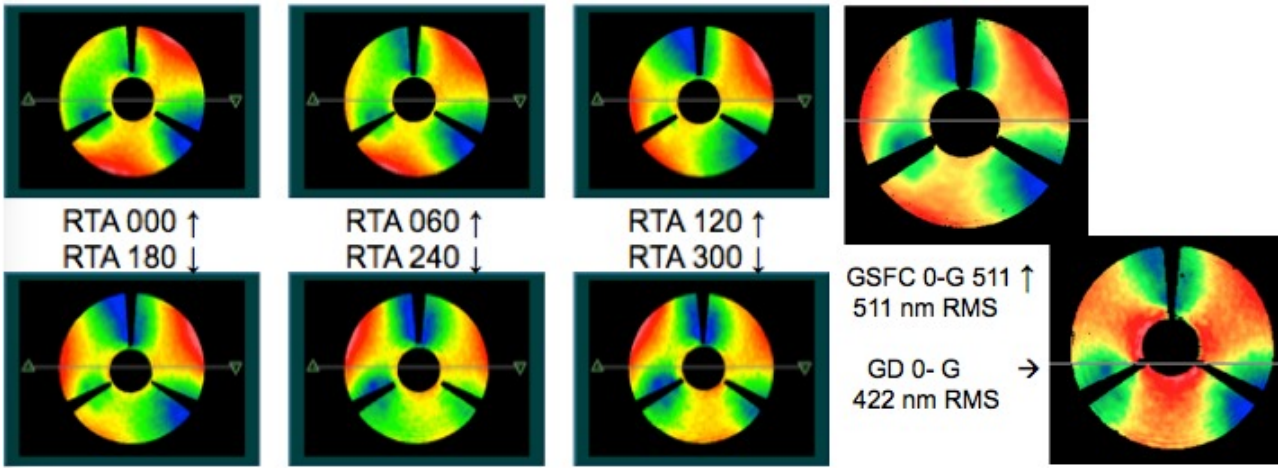

Figure 4. RTA 180-degree clocking pairs and resulting 0-G figure

The estimated zero gravity wavefront error is 511 nm at 632 nm test wavelength which compares favorably to the 422 nm single pass wavefront error measured at General Dynamics (GD) with the gravity offloading system activated. The NASA test was performed with the optical axis of the RTA horizontal, while the GD test is performed with the optical axis vertical. The largest difference between the measurements is due to the uncertainty in the HAF mirror astigmatism; consistent with changes measured after moves during HAF characterization at Arizona Optical Systems. Based on analysis this degree of uncertainty results in changes in the expected encircled energy diameter of less than 1 micron and focal surface position of less than 50 microns. This is within our required accuracy to align the fibers to the RTA focal surface and verify the RTA imaging change due to gravity. In addition, the RTA boresight change in different gravity orientations as within the 0.25 micro Radian allocation.

2.3 RTA focal surface map by interferometry

Mapping of the RTA focal surface using interferometry was required to allow placement of the fiber at their nominal focus position prior to performing plate scale measurements of the RTA. By placing the optical fibers on the focal surface we ensure that the plate scale measurements are not biased by defocused images. In order to determine the

placement of the science fibers along the optical axis relative to the aft optics assembly mechanical datum surface, we determined the offset between the zero power position of the interferometer at each field point and clocking orientation. This offset and clocking orientation is established by using of the BAF surface and the BAF removable tooling balls. Clocking of the RTA allowed characterization of the zero gravity focal-surface and an evaluation of the expected change from the 1 G orientation. Reporting of the interferometrically determined focal surface and the difference measured by minimum encircled energy is deferred to Section 2.6, but was found to be less than 100 microns.

2.4 Setting Focal Plane Plate (FPP) focus

RTA focus was determined using the focal surface mapping performed with the interferometer offset for the difference between the interferometer test wavelength of 634 nm and the nominal laser wavelength of 532 nm. Interferometry was performed measuring the null power position relative to the known ball focus position on the ball plate for each field point and orientation. Knowledge of the diamond turned BAF surface, the AOA datum surface and the measured null produced extremely repeatable and consistent results with very little change in focus with orientation. The six ATLAS science fibers can be individually positioned and shimmed on the focal plane plate. In addition to the science fibers there are two pairs of fibers that reside on the focal plane plate that serve anchor are used to establish the receiver pointing as measured by the Laser Reference System or LRS. The TAMS fibers positions are illuminated with a light source and anchor the Transmitter Alignment Metrology System (TAMS) used as feedback to steer the laser beams. Measurements of plate scale are sensitive to the focus position of the fibers; therefore it was considered prudent to adjust the fibers in focus prior to measuring the RTA plate scale and focal length. The fibers are mounted into ultra precision AVIMS adapters developed by NASA GSFC that reside on the focal plane plate. The AVIMS adapters were shimmed to the focus determined by interferometry and were initially placed at the nominal horizontal and vertical offsets relative to the ATLAS coordinate system. Transverse position characterization of the AVIMS adapters was performed using a Leica MicroVu optical coordinate measuring machine after a local focal plane coordinate system was established. The ATLAS focal plane plate being configured for measurements with the Leica system is shown in Figure 5. A reference edge on one side the focal plane plate is used to define one axis of the coordinate system and an orthogonal axis is defined, the focal plane plate plane is measured and a normal vector created that defines the third orthogonal axis. The origin of the coordinate system is at the central hole on the focal plane plate. Once this coordinate system is defined the LEICA displays the position of the center of the image in the field of view. The use of high magnification and adaptive lighting on the LEICA allowed placement of the AVIMS adapters to better than 5 microns accuracy in each degree of freedom.

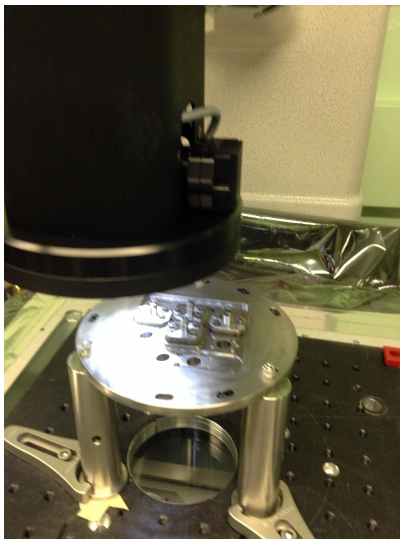
Figure 5. ATLAS FPP on Leica

2.5 RTA plate scale and f# determination

The focal plane plate was installed on the ATLAS RTA and six engineering unit fibers were illuminated using an LED source centered around the nominal wavelength, illuminating a 6 port-integrating sphere. Two Leica T3000 theodolites were aligned to the RTA to view the back-illuminated fibers to determine their angular offset of each channel to allow plate scale determination. CCD cameras were installed on the back of the theodolites to allow magnified viewing of the back-illuminated images and the theodolite reticles. The Leica theodolites are first-order instruments capable of arc second readings but these instruments are not usually thought to be capable of measuring to 0.2-arc second (1 micro-Radian) accuracy. The ATLAS field points are however, only about $\pm$ 0.5 degrees off-axis in the vertical and horizontal axes, within range of higher encoder accuracy in the theodolites. A view of the test configuration is shown in Figure 6. Using the Leica measured positions of the optical fibers and the

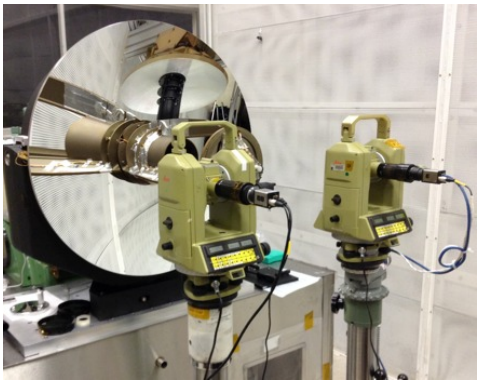
Figure 6. Plate scale determination

resulting angles measured by the theodolites we determined the plate scale to be 277.3 and 277.4 micro Radians/mm on the two instruments with a standard deviation of 0.5 micro Radians. This results in an average focal length of 3.605 meters with a range of 3.597 to 3.614 meters, the average is well within the specification tolerance of 0.5% of 3.6 meters ± .065 meters. The plate scale was measured with the RTA clocked at 0 and 180 degrees with no statistically significant difference in the plate scale. Characterization of the spare unit #2 RTA determined that its focal length was also within specifications but only at the cost of having a back focal distance that was out of specification by 4 mm; enough to cause a physical interference with the focal plane plate. Fortunately, the flight unit did not have this error.

2.6 Encircled Energy

The ATLAS RTA encircled is a measure of how tightly light is focused, which determines the margin between the field of view of the ATLAS science fibers (83 micro Radians and 300 microns diameter in physical space) and the size of the images. Testing at the telescope vendor using double pass interferometry underscored the difficulty in translating between wavefront error and encircled energy. In the case of the ATLAS primary, spindle-wobble during diamond turning of the primary mirror produced mid frequency figure errors that were not completely polished out. Our interferometer did not have the spatial resolution to capture the mid frequency error without zooming and stitching across the aperture a somewhat difficult process. Therefore, the encircled energy measurements performed at the RTA level of assembly; in conjunction with interferometry using sub aperture analysis give the best understanding of this key requirement. ATLAS has modest performance requirements due to the oversized receiver field of view. Testing at the vendor determined that the 80% encircled energy diameter would approach 85 microns; significantly worse than the original specification, but still acceptable. It was further determined that existing optical ground support equipment could be used for testing; specifically a 40" diameter parabolic mirror could be used to build a collimator for testing the ATLAS RTA. The arrangement for the collimator is shown in Figure 7; it consists of the large parabola, an elliptical fold mirror and a source table. The 40" diameter parabola figure was measured at the center of curvature using an interferometer, as was the elliptical fold mirror to allow a model of the collimator to be created. The reference for the collimator primary mirror boresight is the back surface of the mirror, which allows for a repeatable alignment reference.

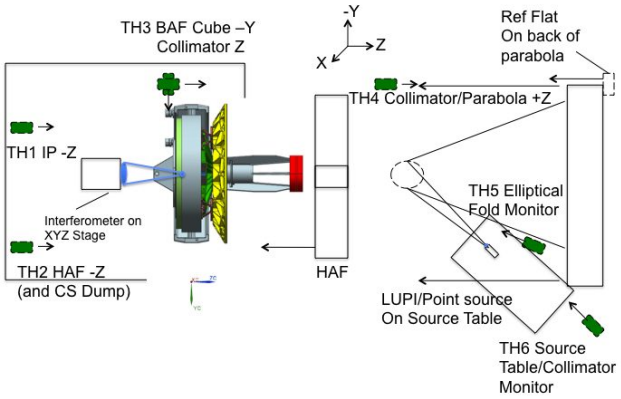

Figure 7. RTA and collimator configuration for Encircled Energy testing

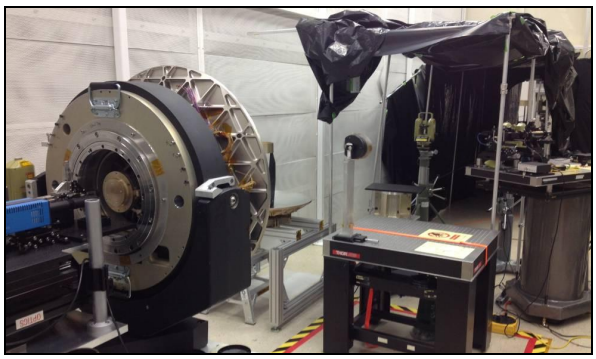

Figure 7,8. RTA viewing collimator & Source

The source table is configured to allow illumination of the parabola with a LUPI compact interferometer for characterization of the system in a double pass configuration using another piece of heritage GSE called the Horizontal Auto collimating Flat (HAF). The HAF mirror is 36" in diameter and was measured at Arizona Optical Systems prior to use on ATLAS. Testing of the ATLAS RTA with the collimator requires periodic characterization to satisfy critical GSE requirements. The collimator is deemed aligned and certified when the minimum wavefront error and power condition is achieved. At this point a precision tooling ball is translated into position and adjusted until it is nulled to the interferometer, providing a useful reference. The tooling ball, resides on a two-axis stage that also holds

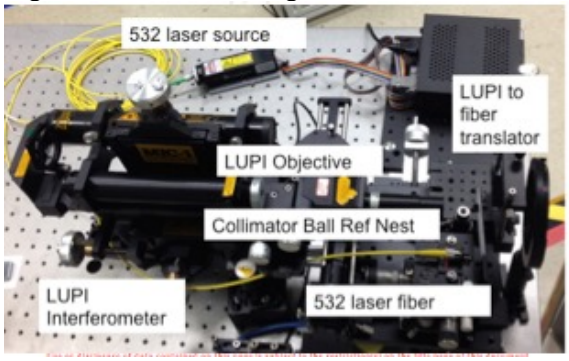

our 532 nm fiber sources and collimator-imaging camera. For encircled energy measurements the precision tooling ball is translated out of position and the launch fiber is translated into position, a theodolite viewing the collimated LUPI laser beam acquires the single mode fiber, which is translated to the same boresight angle as the interferometer point source. Focus of the fiber is achieved by retro reflecting the maximum amount of energy back into the fiber off of the HAF mirror. Once the collimated fiber point source is aligned, the HAF mirror is removed allowing the beam to reach the ATLAS RTA in the Gimbal mount. The diamond turned mounting plate is again used to align each RTA field position to the collimator. A photo of the RTA in the gimbal mount viewing the collimator and the source assembly is shown in Figure 8; a camera is behind the RTA and the source table is to the right of the collimator. Three camera configurations were used to measure on and off-axis encircled energy of the RTA. The first approach employed direct viewing of the focal surface with a CCD. The second (shown in Figure 7) required the use of a 2 to 1 relay lens to acquire the off-axis field points due to mechanical interference of the camera with the AVIMS adapters on the focal plane plate. Lastly, miniature pixel fly CCD's configured for use during thermal vacuum testing were used for direct imaging of select on and off axis field points. The PCO camera and relay slightly underestimate the encircled energy due to the relay system, therefore we based our final estimation of the encircled energy on the pixel fly images. The pixel fly CCD array also had the advantage of mounting directly to the Aft Optics Assembly allowing rotation of the RTA and camera array together.

RTA images from the collimator 532-nm single mode fiber source appear in Figure 9 along with a plot of encircled energy as a function of focus for the on-axis position. Focus sweeps were performed at each field point with each camera in each RTA orientation and best-fit focus positions and 80% encircled energy calculations were performed using custom software written in Matlab. The results indicate an average encircled energy of about 77 microns as measured by the PCO but 85 microns measured by the Patina camera with no relay lens. The difference in the average encircled energy and that in RTA rotation 000 and RTA 180 is less than 2 microns in all cases. Estimates of the encircled energy based on offloaded wavefront measurements

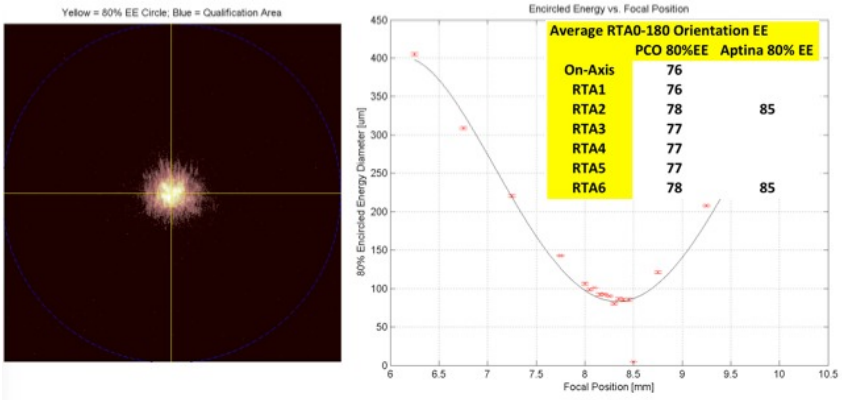

Figure 9. RTA image, focus sweep and encircled energy

of the RTA and sub aperture interferometry to estimate the affect of mid frequency ripple also indicate an encircled energy of 85 microns. This is significantly worse than that expected from the wavefront measurements of the RTA alone. It is interesting to note that the spare RTA primary mirror had significantly less surface error than RTA Unit 1; but did not have improved encircled energy largely due to the uncorrected ripple in the substrates from the common spindle error that was not corrected between RTA builds. In addition to characterizing the encircled energy at each field point, this test measured the offset between the AVIMS datum surface, which controls the focus position of

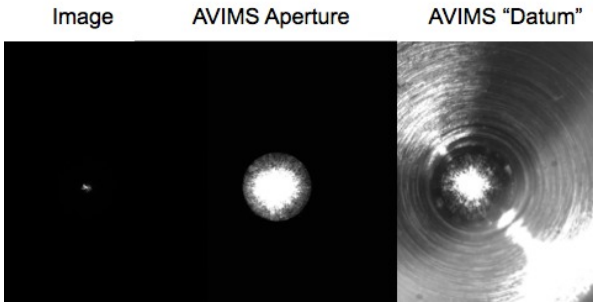

Figure 10. AVIMS imaging and focus DPI offsets

the fiber and the minimum encircled energy focus position. Recall that the AVIMS adapters were set on the focal plane plate using the focal surface data obtained during focal surface mapping with double pass interferometry (DPI). The offset between the AVIMS datum and the minimum encircled energy position was determined by focusing on the AVIMS datum tooling marks with the PCO camera and 2:1 relay lens and then recording the camera translator position. A composite photo

Average RTA0-180 Orientation EE			AVIMS to EE
	PCO 80%EE	Aptina 80% EE	Offset (mm)
On-Axis	76		N/A
RTA1	76		0.069
RTA2	78	85	0.109
RTA3	77		0.075
RTA4	77		0.055
RTA5	77		0.06
RTA6	78	85	0.096

of the RTA image, back-illuminated AVIMS aperture and AVIMS datum is shown in Figure 10. The repeatability of focus on the surfaces is approximately 50 microns. Then the RTA image relayed to the camera, which is again translated in focus to achieve the minimum spot size. The results shown in Figure 11 indicate a worst-case defocus of 109 microns between the AVIMS datum surface and the best encircled energy (EE) focus. This error can be removed by adjusting the focal plane global shim by the average offset of 77 microns. Even without correction, errors in focus of 100 microns affect the encircled energy by less than 1%.

3. ATLAS RECEIVER TO TRANSMITTER BORESIGHT ALIGNMENT

The ATLAS Receiver Telescope Assembly fibers in the telescope focal plane must collect light from the transmitter reflected from the ground and deliver it to the photomultiplier tubes for detection. The transmitter beam direction is determined by laser alignment and the alignment and characteristics of the diffractive optical element or DOE. The DOE is a holographic element that diffracts the laser beam into multiple spots separated by 6.61 milli Radians in the ATLAS-Y axis (horizontal) and 5.0 milli Radians in the ATLAS-X axis. There are many orders diffracted but most of the light is diffracted into 3 high power spots and 3 lower power spots with a ratio of about 4:1 for high to low power. A drawing of the DOE in its clocking adjustable mount and reference cube is shown Figure 11. The AVIMS adapters that hold the receiver fibers in the RTA focal plane must be adjusted to center the field of view of each fiber on the position of the transmitted, Tx laser beams. The angular extent of the receiver fibers is nominally 83 micro Radians, while the nominal size of the laser beam on the ground is approximately 21-micro Radians. Common path alignment errors between the 6 transmitted spots and the receiver can be corrected using the Beam Steering Mechanism (BSM) to steer the laser angle using the Laser Reference System (LRS) for feedback. The six diffracted laser beams coming out of the DOE pass through the Transmitter Lateral Translation Retro reflector (LTR) that splits a small fraction of the power and directs it to the LRS, which determines the transmitter pointing relative to a reference pattern that represents the receiver. There are 6 science fibers within the ATLAS RTA focal plane that collect the light reflected from the Earth; there are also 4 fibers that are connected to a light source of a slightly different wavelength than the laser. The fibers, and light source are also part of the Transmitter Alignment Monitoring System or TAMS. The normal mode is for the TAMS fibers to be illuminated in the RTA focal plane. The RTA projects the beams into collimated space at known angles. The beams are sampled by a TAMS LTR, which picks off a small portion of the RTA aperture and directs it to the LRS. The LRS software performs centroiding of the six laser spots to determine transmitter angle relative to the four TAMS centroids. During instrument calibration, the relationship between the transmitter and receiver alignment is calibrated and a nominal offset is determined. During flight the software will continuously measure these ten spots to determine how to adjust the Beam Steering Mirror (BSM) to keep the transmitter aligned to the receiver. The BSM can only correct for common path alignment errors between the transmitter and receiver. The BSM cannot correct for errors that prevent a perfect overlay between the six spots such as clocking of the pattern, magnification of the pattern (due to errors in fabrication or laser wavelength change) or channel-to-channel misalignment of the pattern. Therefore it is critical to characterize the DOE divergence of the laser beams and align the six AVIMS adapters in the RTA to within 10 micro Radians of each transmitter channel. The LRS control system corrects for common errors due to integration, gravity release, thermal conditions on-orbit and other errors. Clocking of the DOE and tip/tilt of the DOE from nominal can also cause uncorrectable channel-to-channel alignment errors. The purpose of the receiver to transmitter boresight alignment is to minimize the uncorrectable alignment errors and demonstrate margin that is consistent with expected changes from ground to on-orbit.

3.1 Diffractive Optical Element Characterization for Transmitter Alignment

Several Diffractive Optical Element (DOE) substrates were created from a master and their efficiency and angular diffraction characteristics were measured and found to be identical and within 1 micro Radian of their nominal angular separation of orders. The flight and spare DOE substrates were then mounted in alignment cells and characterized to prepare for alignment of the DOE to the transmitter path. The DOE (Figure 11) is mounted in a clocking adjustable cell that has a removable reference cube to facilitate alignment to the instrument. During testing the DOE was illuminated with a surrogate laser, which was controlled to within 0.1 nm of the nominal flight wavelength. A theodolite was then aligned normal to the

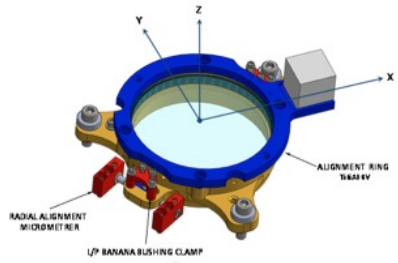

Figure 11. DOE in its mount

DOE and was used to image and measure the angular position of the 6 diffracted science field positions and the zero order beam. The DOE was clocked to level the imaged DOE spots and the higher order spots in the theodolite so they had the same measured elevation. Utilization of the diffracted higher order spots allows for more accurate leveling of the DOE. Once the DOE is clocked to level the higher order spots, a second theodolite is used to measure the elevation of a reference cube mounted on the DOE cell to allow clocking alignment during integration. Since the theodolite elevation is referenced to gravity this allows the DOE clocking to be very accurately set when the DOE is aligned to the ATLAS coordinate system.

3.2 AVIMS Adapter Pre-alignment

Characterization of the expected transmitter channel angles at the DOE level of assembly allows the creation of a nominal receiver angular map. The plate scale determination in Section 2.5 was used to calculate the nominal positions for the center of each fiber in the RTA focal plane. The focal plane plate was installed in the Leica micro-vu coordinate measuring system for alignment of the AVIMS fibers. By creating a local coordinate system for the RTA focal plane plate that utilized a central hole as the origin, a linear feature along the X-axis, a nominal rectilinear position for each science channel fiber can be calculated. In addition, the focal plane plate has an alignment cube that was referenced to the common X-axis reference datum for clocking of the focal plane plate to align to tight tolerances. This datum was transferred to the alignment reference cube by pressing a parallel against the datum and viewing the normal with a theodolite. The focal plane plate reference cube was measured to determine its clocking offset for use during focal plane plate alignment to the RTA. Illumination of the AVIMS adapters from below the focal plane allowed for very accurate determination of the center of the fiber in the local coordinate system. It was possible to adjust the AVIMS positions to better than 5 microns by loosening the fasteners and sliding the adapters on the interface and tightening them down. The purpose of this pre-alignment was to place the adapters close to nominal to limit the amount of adjustment required.

3.3 AVIMS final alignment using ETU DOE and Flight RTA

In order to reduce schedule and technical risk we performed what became the final alignment of the receiver science channels at the RTA level of assembly. This was accomplished using the 40-inch diameter collimator system that imaged the back illuminated science fibers in the RTA focal plane and the DOE transmitter channels. The optical configuration is shown in Figure 12. First the focal plane plate was installed on the Aft Optics Assembly on the back of the RTA; its centration and clocking is constrained by 3 alignment pins on the AOA. The RTA was then clocked in the gimbal mount until the focal plane plate reference cube was at a clocking elevation that would result in science channels that were level as determined during focal plane pre-alignment. The ETU DOE and proxy laser were then installed on the RTA gimbal mount. The RTA gimbal mount allows precise adjustment of the RTA boresight in azimuth and elevation using the diamond turned reference plate as an alignment reference of the RTA boresight. The DOE normal was aligned to the RTA boresight using a theodolite to minimize asymmetry of the diffracted beams due to striking the DOE at an off-nominal angle. The DOE was also clocked to its nominal rotation using a theodolite to view the reference cube on its mount that was measured during DOE characterization. The proxy laser was adjusted in tip/tilt until the zero-order image was near the nominal offset angle with respect to the RTA boresight as determined by a theodolite. Engineering unit fibers were installed to the AVIMS adapters on the RTA focal plane and illuminated by a diode laser centered near the nominal wavelength of 532 nm. The gimbal mount was then adjusted in tip/tilt to place science channel 5 of the RTA on the

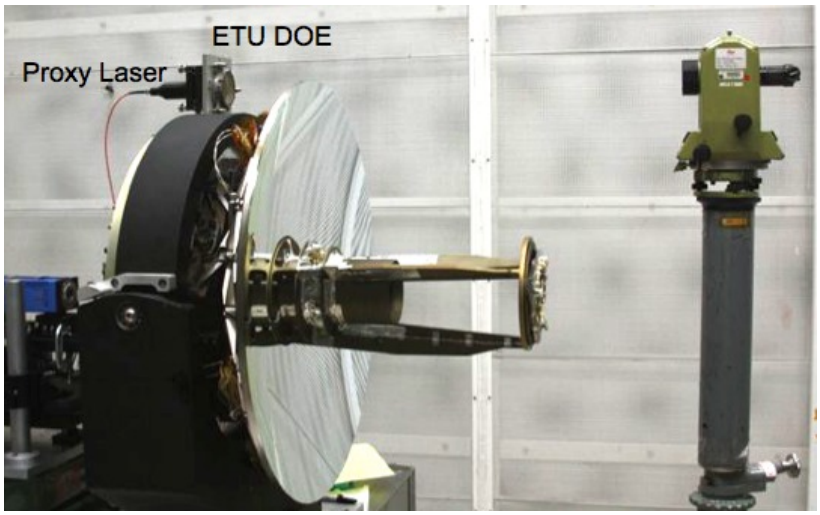

Figure 12. Imaging of back illuminated RTA and DOE in collimator

collimator boresight where it could be imaged in the collimator focal plane by a Basler CCD camera with 12-bit digitization. The proxy laser was then illuminated and the DOE Transmitter (Tx) spot corresponding with science channel 5 was viewed in the collimator focal plane and the laser adjusted in tip/tilt to superimpose it on the image of the back illuminated fiber in science channel 5 Receiver (Rx) spot. An intentional azimuth offset was then introduced between the Tx and Rx to allow centroiding between the two spots to be performed. Fifty images of the separated spots were acquired using the acquisition software for the camera. The gimbal was then adjusted to view and determine the Tx to Rx offset for each channel and the images saved. Figure 13 shows the Tx and Rx images and illustrates the

difference in the size of the Tx and Rx spots and shows the standard deviation in the centroiding of the images to be at the single micro Radian level. Image J software was utilized to centroid on the individual Tx and Rx spots for each frame and an average horizontal and vertical pixel position was determined along with the standard deviation of the centroids. The data was then adjusted for the collimator plate scale to convert the Tx to Rx offsets to micro Radians. The average offset in the ATLAS horizontal (Y axis) and vertical (X axis) for all 6 spots was then calculated to determine the "group offset". Since ATLAS has a beam steering mirror (BSM) the group offset can be corrected at the instrument level. A simulation of this "realignment" can be performed analytically by subtracting the average Y and X angles from the measured position for each channel. The RTA was then clocked 180 degrees, the process repeated and the difference in the boresight offset between channels in the two orientations calculated to determine if a gravity offset was required. The change was found to be within the measurement error of 1 micro Radian and therefore not compensated. The uncorrectable Tx to Rx boresight error for each channel is shown in Figure 14. The goal was to achieve better than 10 micro Radians of co-alignment; this was not achieved because the pincushion distortion of the RTA was not taken into account during the AVIMS adapter alignment. Therefore, adjustment of the AVIMS adapters moving them to co-align the images was performed as an alternative to additional alignment using the micro Vu system. This had the added benefit of path finding the approach that would be used at the instrument level of assembly should further realignment be required.

Figure 13. Rx and Tx images

Transmitter to Receiver Boresight Error					
RTA1 Error		RTA3 Error		RTA5 Error	
Y micro Rad	X micro Rad	Y micro Rad	X micro Rad	Y micro Rad	X micro Rad
5.4	-6.0	1.8	-11.1	1.3	-4.9
Radial Error	8.1	Radial Error	11.2	Radial Error	5.0
RTA1 Error		RTA3 Error		RTA5 Error	
Y micro Rad	X micro Rad	Y micro Rad	X micro Rad	Y micro Rad	X micro Rad
5.8	5.1	-3.7	14.2	-2.0	6.6
Radial Error	7.7	Radial Error	14.6	Radial Error	6.9

Figure 14. Tx to Rx Boresight Error

3.4 AVIMS adapter in-situ alignment on RTA focal plane at the RTA level of assembly

A channel-by-channel adjustment of the AVIMS adapters to center the Rx (back illuminated science fibers) image on the corresponding DOE channel was performed. This was accomplished by adjusting the proxy laser to superimpose the Tx to the Rx on channel 5 as viewed in the collimator focal plane by the Basler camera. The AVIMS bolts were loosened and the adapters were manually translated on the focal plane in the vertical and horizontal axes to minimize the offset between the Tx and Rx in both axes. After each AVIMS was adjusted a set of fifty Tx and Rx images were taken for each channel, centroids calculated and the group average and uncorrectable error determined. Figure 15 shows the Tx to Rx boresight error in the Y and X axes after common error subtraction and the resulting radial offset from nominal to be less than 3 micro Radians for each channel. A composite image of all Tx and Rx overlapped channels is also shown. RTA level alignment of

Final RTA Level Transmitter to Receiver Boresight Error					
RTA1 Error		RTA3 Error		RTA5 Error	
Y micro Rad	X micro Rad	Y micro Rad	X micro Rad	Y micro Rad	X micro Rad
-0.4	0.1	0.1	-0.6	-0.7	2.7
Radial Error	0.4	Radial Error	0.6	Radial Error	2.8
RTA1 Error		RTA3 Error		RTA5 Error	
Y micro Rad	X micro Rad	Y micro Rad	X micro Rad	Y micro Rad	X micro Rad
0.8	-0.5	-0.2	-3.0	0.4	-0.9
Radial Error	0.9	Radial Error	3.0	Radial Error	0.9

Figure 15. Tx to Rx Boresight and images

Composite image of overlapped Tx and Rx Images

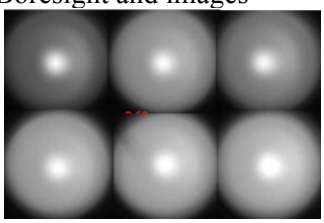

the Tx to Rx spots does not ensure that the alignment will be optimized at the instrument level. An assessment of expected changes of the Tx and Rx alignment due to various contributors was performed and the conclusion is that less than 4 micro Radians of change is expected from the RTA level of assembly to the instrument level throughout integration and environmental testing.

4. INSTRUMENT LEVEL ALIGNMENT

The ATLAS Optical Bench (OB) was fabricated at the Goddard Space Flight Center and consists of an aluminum core with composite panels epoxied to the core. This structural panel was machined to accommodate titanium fittings that allow integration of the instrument components on the Optical Bench. The primary datum that defines the ATLAS coordinate system is the RTA interface plane defined by the 3 pads and pins that control the RTA alignment. A drawing of the RTA on the optical bench is shown in Figure 16. The RTA datum is controlled to 0.0005" to minimize mounting strain to the RTA flexures. Testing of the telescope at General Dynamics and Structural Thermal OPtical (STOP) modeling at GSFC determined that this co-planarity was adequate for the RTA. The ATLAS Optical Bench coordinate system was established during CMM characterization at GSFC using the RTA interface datum normal to establish the Z axis, the line between two of the RTA alignment pins was used to determine the Y axis and the X axis was set normal to Z and Y. The origin of the coordinate system is at the center of the RTA hole on the Optics Bench at the intersection with the Z plane defined by the RTA interface inserts. This coordinate system was determined and then transferred to fittings and cubes on the Optics Bench that are visible throughout I&T. Since the Optics Bench is sequentially loaded with many subsystems it is critical that the alignment of each subsystem and characterization of the instrument coordinate system with gravity orientation be performed.

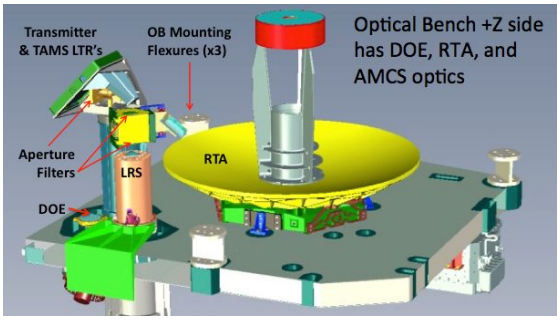

Figure 16. +Z face of ATLAS OB

4.1 DOE alignment to the ATLAS instrument

The DOE diffracts the light from the ATLAS lasers located on the other side of the optical bench to produce the six transmitter beams that are projected to the Earth and viewed by the RTA to determine surface topology. The DOE is installed on the ATLAS optics bench and clocked to the nominal angle to level the 6 transmitter beams to the ATLAS optical axis. During the DOE characterization the nominal clocking angle of the DOE was determined and referenced to the alignment cube. The DOE was installed on the optics bench and clocked to the nominal angle with respect to the ATLAS coordinate system to within 10 arc seconds to achieve a similar alignment relative to the RTA as was achieved during RTA level testing.

4.2 Laser Alignment to ATLAS Instrument

There are two lasers on the ATLAS instrument that reside on the optics bench –Z side; only a single laser is used at any time to provide the transmitter pulses. The lasers were fabricated by FiberTek and characterized prior to delivery to NASA. They were aligned to a nominal mechanical position on the ATLAS bench using laser trackers and theodolites to place the laser beam within its allocated alignment tolerance of 100 micro Radians. Laser 1 is folded into the transmitter path by a fold mirror (FM) and Laser 2 by a polarization beam combiner (PBC). The beams are expanded by the reflective Beam Expander (BE) and then folded to pass through the DOE and exit along the +Z axis by the Beam Steering Mirror (BSM). During alignment the lasers are energized and a pair of on-board Risley prisms adjusted to center the laser beams on the DOE aperture as viewed through a series of filters by a CCD camera. The BSM is then adjusted to align the laser beam to its nominal boresight angle relative to the ATLAS Receiver.

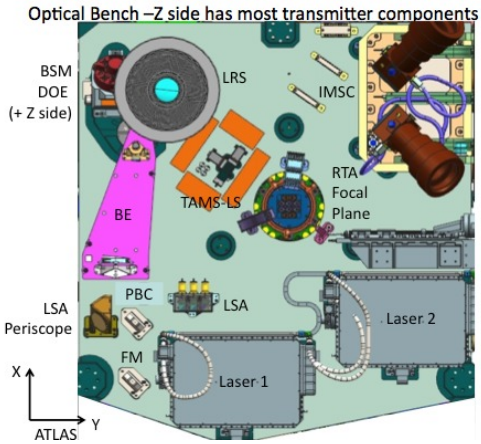

Figure 17. ATLAS OB –Z Components

4.3 ATLAS RTA focal plane plate alignment

During focal plane characterization and alignment, the clocking angle of the focal plane plate (FPP) was measured and transferred to the FPP alignment cube. The ATLAS focal plane plate was installed on the Aft Optics of the RTA to a nominal clocking angle to level the Receiver fibers to the ATLAS coordinate system. The clocking angle of the FPP was adjusted to compensate the residual clocking angle remaining after DOE to minimize the clocking offset of the Tx to Rx channel group. It is important to note that the AOA has alignment pins that control the centration of the FPP, but that the FPP has slots to allow clocking of to accomplish this alignment prior to torqueing the bolts to secure the FPP. After verification that the alignment is correct, epoxy is used to stake the interface to prevent rotation due to thermal or launch loads.

4.4 ATLAS Instrument Level Tx to Rx Co-boresight Alignment Verification

The ATLAS channel-to-channel Transmitter to Receiver co-boresight alignment is verified at the instrument level at several key points during instrument qualification. The initial test is essentially a repeat of testing done at the RTA level of assembly with the collimator imaging the Transmitter channels and the back illuminated RTA science channels. Due to the high laser power the transmitted laser beam is attenuated with the Laser Optical Attenuation System (LOAS). A view of the RTA integrated to the ATLAS instrument structure is shown in Figure 18. The ATLAS instrument is aligned to the collimator optical axis and then each viewed in the collimator focal plane using the CCD camera as seen in Figure 19. The instrument level test is performed with the flight lasers, flight DOE, flight fibers and with the RTA integrated to the fully loaded optical bench. In addition to viewing the transmitter and receiver images in the collimator focal plane, we were able to view the highly attenuated transmitter spots with a theodolite outfitted with a theodolite to determine the group pointing relative to the ATLAS coordinate system. An image of two of the high power and two of the low power laser spots and the zero order spot is shown in Figure 20. The higher order diffracted images are also visible. We expect small changes from the lower level of assembly testing due to the laser wavelength, differences in the fibers, DOE, and clocking errors in the DOE and focal plane. Testing of the channel-to-channel alignment at the instrument level indicates that the co-boresight error is within 3 micro Radians for each channel in this flight configuration. Testing was repeated after instrument level vibration that found to co-boresight error be unchanged to within the measurement uncertainty for both lasers. A summary of the

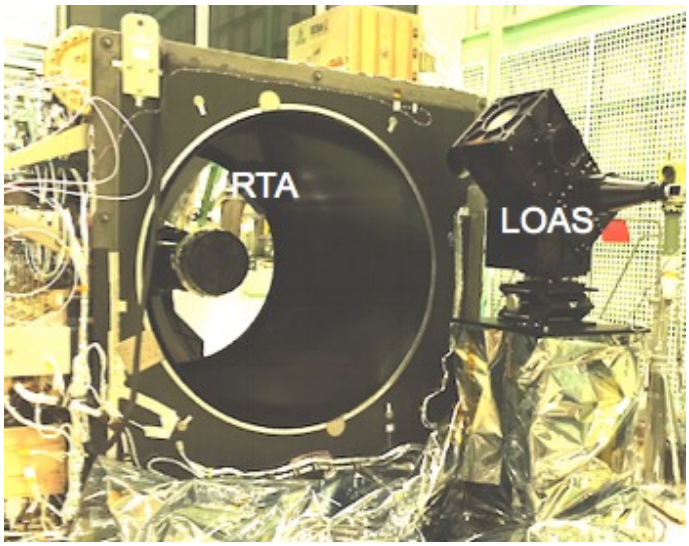

Figure 18. ATLAS RTA at Instrument Level

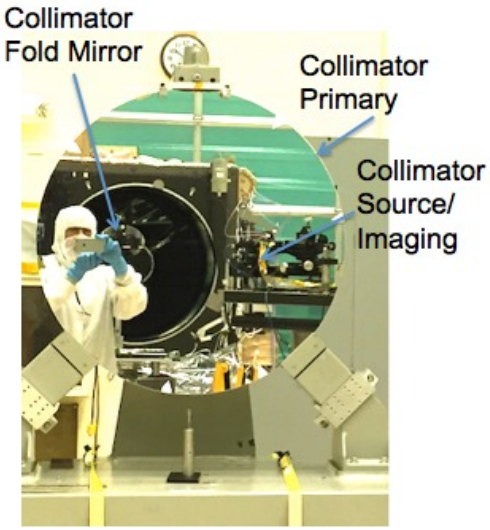

Figure 19. ATLAS Collimator Primary

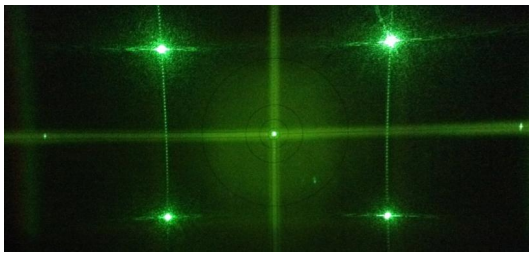
Figure 20. Transmitter Images

expected error between the Tx and Rx channels due to configuration changes in shown in Figure 21. The measured co-boresight error is within that predicted due to changes in hardware and configuration.

Contributor	Status	Included In RTA Test	Verification	Instrument Level Risk
Clocking of Focal Plane Plate	<1 micro-Radian	Yes	Theodolite	Low
Clocking of of DOE	<1 micro-Radian	Yes	Theodolite	Low
AVIMS sleeve to bore non-concentricity	15- 20 micron error	Yes	Micro-Vue CMM	Low
Deviation from predicted field distortion	2 microns	Yes	Field Map w/camera	Low
Gravity offloading (clock RTA 180)	1 micro-Radian	Yes	Field Map w/camera	Low
AVIMS repeatability	< 1 micro-Radian	No	Repeatability test	Low
DOE tip/tilt error at RTA level of testing	1 micro-Radian	No	DOE test	Low
Swap from GSE to flight fibers	< 3 micro-Radian	No	Based on Flight Fiber Data	Low
Environmental effects	< 2 micro-Raidan TBR	No	Modeling/Instrument Test	Low
Expected difference at instrument level		4	micro Radians	

Figure 21. Estimated additional co-boresight error at instrument level

Measurement and tracking of the co-boresight alignment using the collimator was critical to providing an independent assessment of the transmitter to receiver alignment prior to handoff of this monitoring function to the LRS. As an on-board system the LRS was used to monitor the alignment during ambient testing in preparation for thermal vacuum testing of the instrument as part of the environmental qualification required prior to launch. During Thermal Vacuum (TVAC) testing the instrument is exposed to thermal excursions that go beyond those expected on orbit, these comprise the Hot Qualification and Cold Qualification cases ("Hot Qual" and "Cold Qual"). The LRS provides feedback to the control system to adjust the BSM to realign the transmitter to the receiver as the alignment of the system changes as a function of temperature. A preliminary assessment of the uncorrectable co-boresight error between each channel during these thermal excursions is shown in Figure 22. In all cases the maximum radial error was below 10 micro-Radians demonstrating significant margin for pointing even in the most extreme thermal conditions. The average BSM angular adjustment to perform group realignment was well under 100 micro Radians for these thermal conditions, well within the 1000 micro Radian allocation for on-orbit adjustment.

Laser 1		Max Error - micro Radians		
Channel	Axis	Hot Qual1	Cold Qual1	Hot Qual3
1	Y error	5.9	0.3	-3.9
	X error	5.2	-5.4	3.3
2	Y error	-3.9	-0.7	0.4
	X error	-3.7	-8.8	-4.2
3	Y error	5.6	2.8	-1.6
	X error	1.9	1.4	2.0
4	Y error	-2.7	-1.5	1.1
	X error	-1.2	0.4	-2.1
5	Y error	-3.4	0.2	1.0
	X error	-1.8	4.4	0.0
6	Y error	-1.5	-1.0	3.1
	X error	-0.4	8.0	1.0
		RMS Error		
All	RMS ErrorY	4.5	1.5	2.4
	RMS ErrorX	3.1	6.2	2.8
	Radial	5.5	6.4	3.7
		Max error		
All	Y	5.9	2.8	3.1
	X	5.2	8.0	3.3
	Radial	7.8	8.5	4.5

Laser2		Max Error - micro Radians	
Channel	Axis	Hot Qual2	Cold Qual2
1	Y error	6.4	2.9
	X error	-0.6	-0.6
2	Y error	-3.5	-1.7
	X error	-7.2	-4.3
3	Y error	-1.7	0.7
	X error	1.1	-0.6
4	Y error	-0.8	-1.1
	X error	-1.4	0.0
5	Y error	-1.2	-0.7
	X error	3.1	1.8
6	Y error	0.8	-0.1
	X error	5.0	3.6
		RMS Error	
All	RMS ErrorY	3.4	1.6
	RMS ErrorX	4.2	2.7
	Radial	5.5	3.1
		Max error	
All	Y	6.4	2.9
	X	5.0	3.6
	Radial	8.1	4.6

Figure 22. Uncorrectable Tx to Rx Co-Boresight Error in TVAC

5. CONCLUSIONS

Testing of the ATLAS RTA and supporting analyses verified the salient optical performance requirements including encircled energy, RTA boresight with respect to mechanical datum, boresight stability under gravity loading and focal length. Testing also established the RTA focal surface to enable alignment of the focal plane. Correlation of the interferometrically determined focal surface and minimum encircled energy position agreed to within 100 microns, more than adequate to ensure efficient coupling of the received light into the optical fibers. The f -number and plate scale of the RTA was found to be within requirements based on telescope vendor and NASA testing. The agreement falls within the measurement uncertainty; again this uncertainty was insignificant relative to the requirements. The RTA 0-G wavefront error measured at the telescope vendor and the analytically extrapolated 80% Encircled Energy (EE) did not

meet the initial requirements due to mid frequency ripple of the substrate. Further analysis of system requirements determined that a relaxed encircled energy performance was acceptable if the co-boresight alignment requirements could be met. Measured EE during image testing at GSFC in ambient and thermal vacuum conditions were found to meet the relaxed requirement. The non-correctable co-boresight alignment error of the receiver fiber placement relative to the transmitted laser beams at the instrument level of assembly was less than 3 micro Radians with all indications that the goal of 10 micro Radians channel to channel co-alignment could be maintained on-orbit. Figure 23 pictorially shows the RTA science fiber field of view and the size of the laser spot (laser beam divergence convolved with the RTA encircled energy) imaged through the system relative to the initial requirements. The effect of co-boresight errors due to alignment, gravity and thermal affects is also shown to illustrate the expected margin on-orbit.

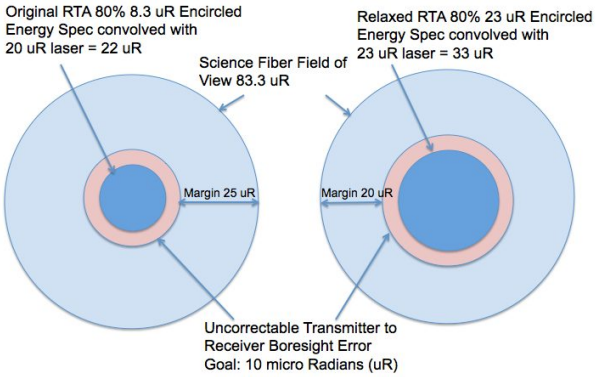

Figure 23. iFOV Rx and Tx spot

REFERENCES

[1] W. Abdalati, H. J. Zwally, R. Bindschadler, B. Csatho, S. L. Farrell, H. A. Fricker, D. Harding, R. Kwok, M. Lefsky, T. Markus, A. Marshak, T. Neumann, S. Palm, B. Schutz, B. Smith, 1. Spinhirne, C. Webb, "The ICESat-2 Laser Altimetry Mission, " Proc. IEEE Vol. 98, No. 5, May 2010.

[2] Hagopian, John G., Evans, Tyler, et.al. "ICESat-2 ATLAS telescope testing"; *IEEE* Aerospace Conference Proceedings 2015 · June 2015.